JOURNAL OF MATERIALS SCIENCE 20 (1985) 4345–4353

Strength characterization of yttria-doped sintered silicon nitride

R. K. GOVILA
Ceramic Materials Department, Ford Motor Company, PO Box 2053, Dearborn, Michigan 48121, USA

The flexural strength of yttria-doped sintered silicon nitride was evaluated as a function of temperature (20 to 1300° C in air environment), applied stress and time. Two mechanistic regimes were manifest in the temperature dependence of the fracture stress. A temperature-independent region of fast fracture (catastrophic crack extension) existed up to 900° C, in which the mode of crack propagation was primarily transgranular. Above 1000° C, the strength (fracture stress) decreased considerably due to the presence of subcritical or slow crack growth which occurred intergranularly. This material did not show a static oxidation problem in short-term ($\leqslant$ 100 h) tests in the low-temperature regime (600 to 1000° C) as has been observed in other yttria-doped silicon nitrides. Flexural-stress rupture testing in the temperature range 800 to 1200° C in air indicated the material's susceptibility to time-dependent failure, and outlines safe applied stress levels for a given temperature.

1. Introduction

Silicon nitride containing yttria in hot-pressed and sintered form is currently being evaluated for use in structural components at high temperatures ($\geqslant$ 1000° C) for gas turbines because of high strength and good thermal shock resistance. Hot-pressed material is limited in commercial use to simple shapes like solid circular discs and rectangular or triangular pieces like cutting-tool inserts. Structural engine components like turbine stators and rotors cannot be fabricated to net shape by hot-pressing methods, and machining from hot-pressed billets is too expensive and time consuming. In contrast, sintered material offers an advantage over the hot-pressed material since many structural components can be fabricated using commercial injection-moulding or slip-casting techniques. Under suitable conditions (time, temperature and pressure), engine parts can be sintered to full density provided allowance is made for sintering shrinkages. This study was undertaken to characterize the strength behaviour of a commercially available yttria-doped sintered silicon nitride (GTE SNW–1000) by evaluating fracture strength as a function of temperature (20 to 1300° C); failure sites and the mode of crack propagation were examined fractographically. In addition, long-term reliability and durability were characterized using flexural-stress rupture testing at several temperatures.

2. Material, specimen preparation and testing

2.1. Material

The material used in this study was yttria-doped sintered silicon nitride commerically known as SNW–1000 (GTE Wesgo Division, Belmont, California 94002) obtained in the form of a rectangular billet of approximate dimensions 100 mm × 100 mm × 37 mm. The sintered silicon nitride contained both yttria and alumina as sintering aids, and had a density of 3 g cm^{-3}. The exact composition is not known due to the proprietary nature of this material; the nominal composition (silicon nitride powder + 13 wt %

0022–2461/85 $03.00 + .12

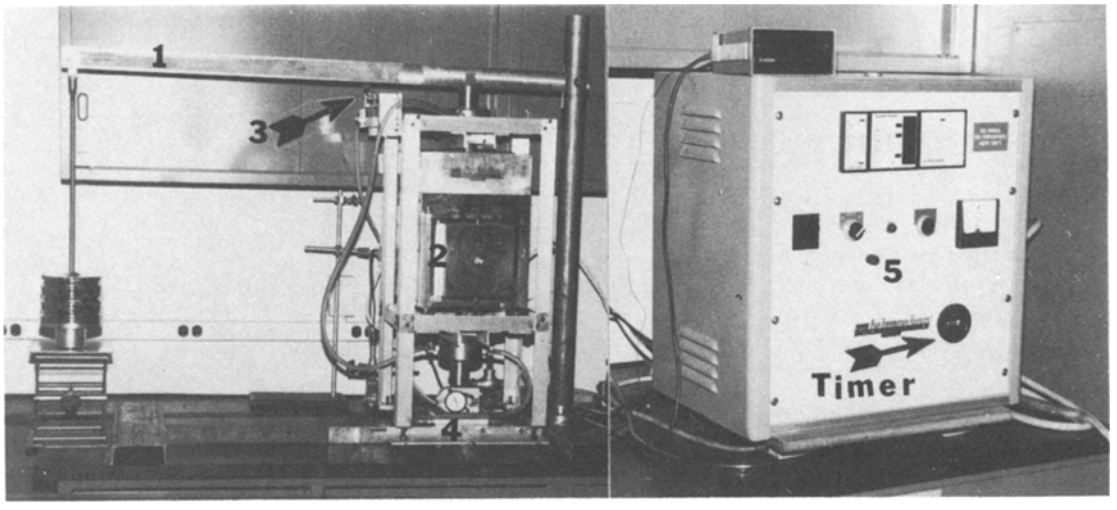

Figure 1 Overall view of the flexural stress rupture test rig: (1) lever arm, (2) furnace, (3) microswitch, (4) load indicator, (5) temperature controller.

Y_2O_3 + 3 wt % Al_2O_3) and other strength properties have recently been reported by Quackenbush and Smith [1].

2.2. Specimen preparation and testing

Flexural test specimens (approximately 32 mm × 6 mm × 3 mm) were machined from the sintered billet. All faces were ground lengthwise using 320 grit diamond wheels; the edges were chamfered (lengthwise) to prevent notch effects.

For flexural strength evaluation, specimens were tested in 1/4-point, four-point bending (inner span is one-half of outer span) in an Instron testing machine (Model 1125) using a specially designed self-aligning ceramic fixture [2] made from hot-pressed SiC. The outer and inner knife edges of the testing fixture were spaced approximately 19 mm and 9.5 mm apart respectively. The high-temperature bend tests were conducted in air using a rapid temperature response furnace attached to the testing machine head. In high-temperature tests, specimens were held at the test temperature for 15 min to achieve equilibrium before testing was begun. No preload was applied on test specimens for either room-temperature or high-temperature tests. All specimens were tested at a machine crosshead speed (MCS) of 0.5 mm min^{-1}, which is considered a fast-fracture mode.

The flexural stress rupture tests at elevated temperatures (800 to 1200° C) in air environment were also conducted in four-point bending using the self-aligning ceramic fixture and furnace. The load was applied to the test specimen through a lever-arm, dead-weight type assembly. The experimental set-up was equipped with a microswitch to cut off power to the furnace and the timer at the instant specimen failure occurred. The total time to failure was recorded. An overall view of the test set-up is shown in Fig. 1, and complete details regarding the design and operation of the stress-rupture test rig are given elsewhere [3].

3. Results and discussion

3.1. Chemical composition and phases

Yttria-doped silicon nitride prepared either by hot-pressing or sintering methods is extremely sensitive to chemical impurities or additives in influencing its mechanical strength properties. In particular, the addition of Al_2O_3 has a wide range of effects, namely in improving densification, lowering sintering and hot-pressing temperatures, and preventing or reducing oxidation at intermediate temperatures (600° to 1000° C). Some disadvantages include suppressing crystallization of the intergranular phase and promoting its presence as an amorphous phase, and lowering of the high-temperature (> 1000° C) fracture strength due to glass formation or promoting subcritical crack growth and rapid oxidation. The effects of Al_2O_3 addition in silicon nitride powder are well discussed by Smith and Quackenbush [4, 5].

X-ray diffraction taken of the as-machined

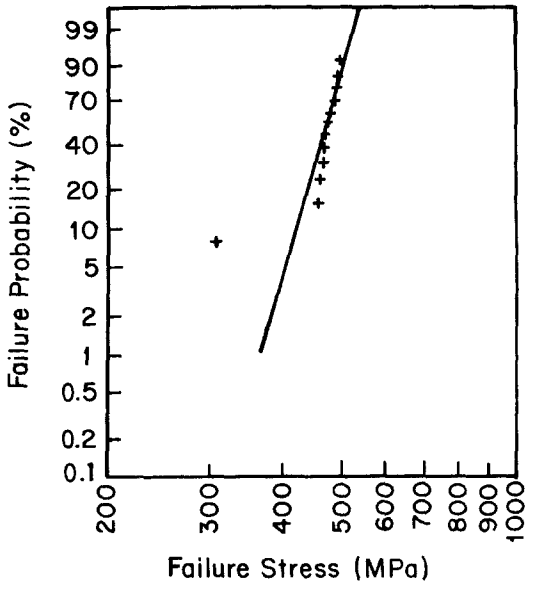

Figure 2 Statistical variation in fracture strength at 20° C for sintered silicon nitride (SNW–1000).

bulk sample revealed primarily β-Si_3N_4. It appears that the presence of Al_2O_3 suppressed crystallization of the intergranular Y–Si–O–N phases. In the absence of Al_2O_3 (or containing small amounts of $\leqslant 1\%$), yttria-doped silicon nitride shows the presence of several secondary phases such as $Y_2Si_3O_3N_4$, $Y_5Si_3O_{12}N$ (H-phase), $YSiO_2N$ (K-phase), and $Y_4Si_2O_7N_2$ (J-phase). These phases are usually intergranularly dispersed in β-Si_3N_4 matrix, and control particularly the high-temperature strength of the material. In addition, all of these phases are susceptible to oxidation with varying degrees of molar volume changes, and thus degrade the materials strength as discussed by Smith and Quackenbush [4, 5], Lange [6] and others [7, 8].

3.2. Flexural strength and its variation with temperature.

At room temperature, a total of twelve specimens were tested in four-point bending to determine the fast-fracture strength. A typical statistical variation in fracture strength, σ_F, at 20° C is shown in Fig. 2. The σ_F varied from a minimum of 307 MPa* to a maximum of 505 MPa with an average strength of 468 MPa, Weibull slope of 16.5 and a standard deviation of 35 MPa. The high value of Weibull modulus could be due to the small number of samples tested. Another earlier study by Easler, Bradt and Tressler [9] on the same material (SNW–1000) but using a larger data base (50 test samples) and different specimen size† reported an average strength of 420 MPa with a Weibull slope of 8.2. Examination of the fracture surfaces in this study revealed failure-initiating sites as surface and sub-surface porosity, and flaws associated with processing contaminants, such as free silicon and occasionally iron. A typical fracture surface showing failure occurring at an iron inclusion is shown in Fig. 3. From the fractographs, it appears that the primary mode of crack propagation during fast fracture (catastrophic failure) is transgranular. Note the uniform distribution of fine porosity in the material (Figs. 3b and c).

Flexural strength was also evaluated at higher temperatures (800 to 1300° C) and the variation in strength as a function of temperature is shown in Fig. 4. Small variations in σ_F were observed in tests made at 800° C, and σ_F can be considered independent of temperature up to about 900° C. The constancy of σ_F in this temperature range implies that a single fracture mechanism predominates, and that insignificant plastic deformation (viscous flow due to glass formation) accompanied the fracture process.

A sudden and significant increase in σ_F was observed in tests made at 1000° C. This rapid increase in σ_F leading to a peak value‡ (see Fig. 4) indicates blunting of the microcracks or flaws due to viscous flow (softening of the glassy phase). Since these tests were carried out in a fast fracture mode (machine crosshead speed = 0.5 mm min^{-1}) at 1000° C, examination of the fracture surfaces did not reveal the presence of subcritical (slow) crack growth indicative of viscous flow (glass formation). However, flexural stress rupture tests carried out at this temperature (1000° C) clearly indicated the presence of slow crack growth (SCG) as discussed later, and thus confirmed the above hypothesis. At

*This particular specimen showed failure occurring at a large inclusion similar to that seen in Fig. 8(a), which would account for the low strength.

† Test samples were 30 mm × 2.5 mm × 2.5 mm, tested in four-point bending with an outer span of 22.2 mm and inner span of 7.4 mm. A machine cross-head speed of 1.3 mm min^{-1} was used.

‡It should be pointed out that the peak value in σ_F could have occurred anywhere in the range 950 to 1050° C. Since the tests were carried out only at 1000° C, hence it is shown at this temperature.

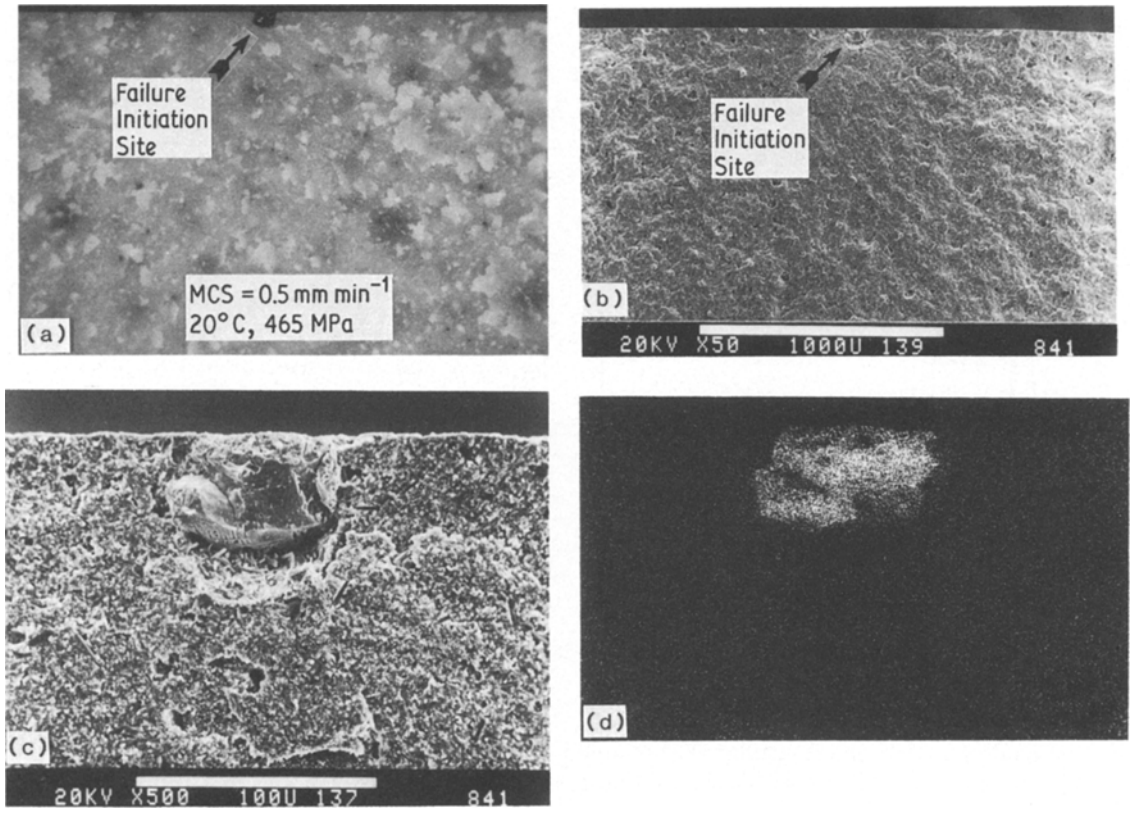

Figure 3 Failure initiation occurring at an inclusion (iron particle) seen optically and in the scanning electron microscope (SEM). (a) Fracture surface in polarized light, magnification × 50. (b) SEM fractograph showing the same areas as seen in (a). (c) SEM view at higher magnification. Cracks surrounding the inclusion are visible. Note distribution of fine porosity in the Si_3N_4 matrix. (d) X-ray map for iron using an energy dispersive spectrometer, illustrating the concentration of iron at the inclusion site. Same magnification as in (c).

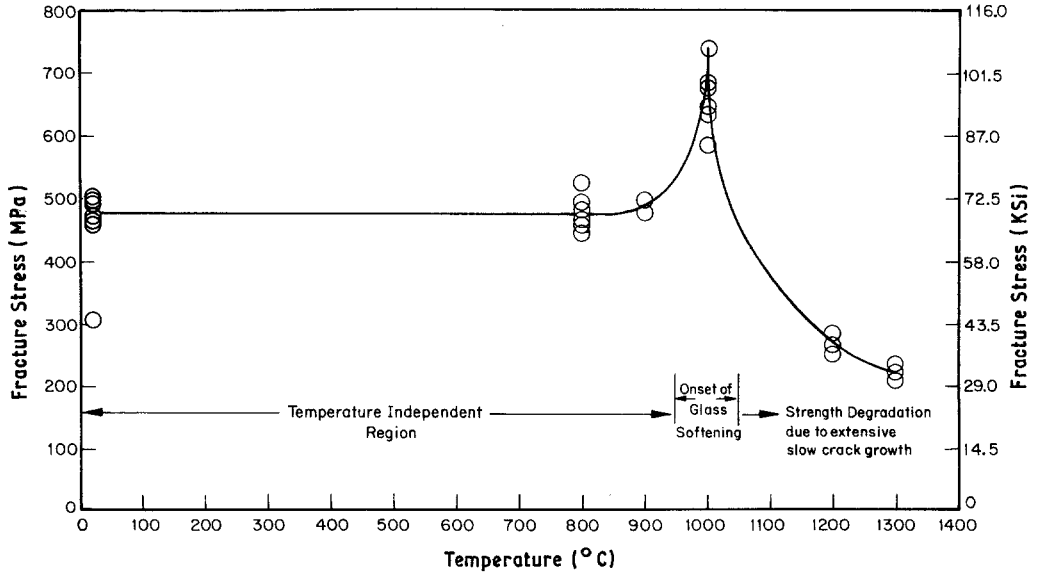

Figure 4 Variation in fracture strength as a function of temperature for sintered silicon nitride (SNW–1000).

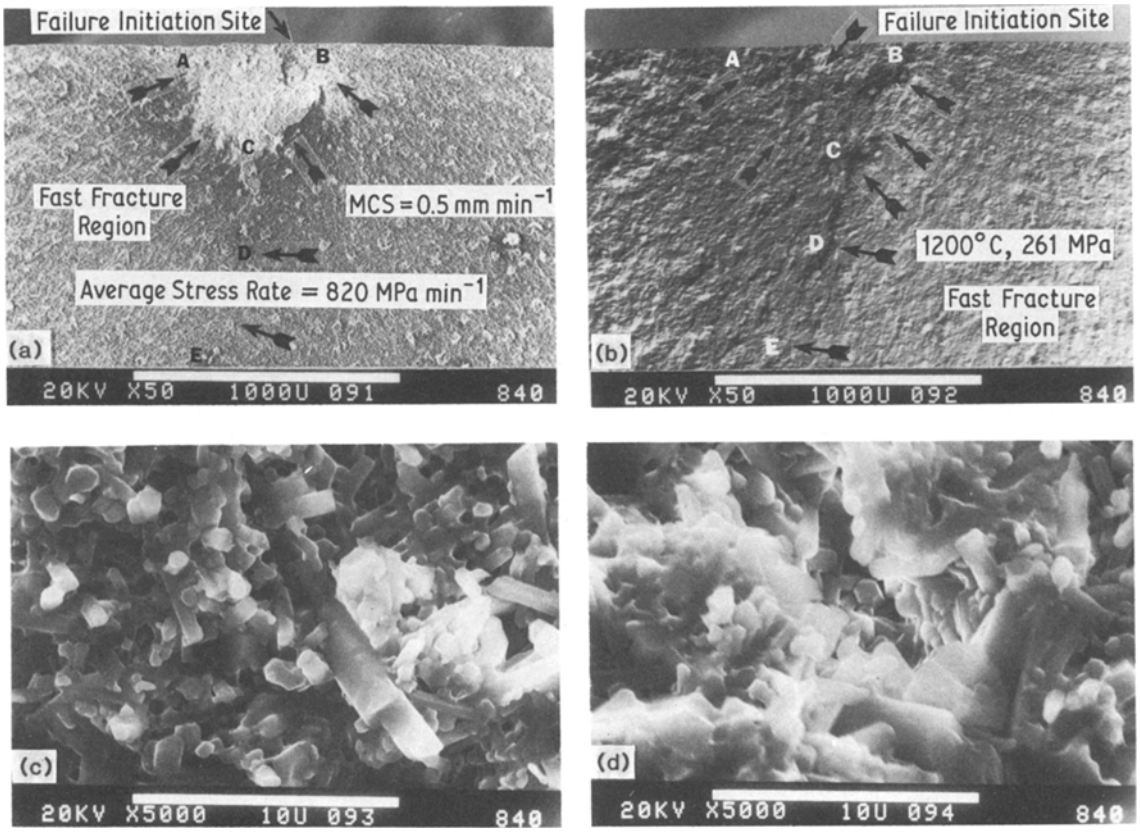

Figure 5 Typical SEM fractograph of SNW–1000 specimen tested in flexure at 1200° C in air. (a) ACB is the slow crack growth (SCG) region. (b) Same area as seen in (a) but in back-scattered mode, illustrating the extent of damage and roughness caused during SCG. CDE is a crack coming out of the SCG zone. (c) Micrograph taken inside the SCG region, illustrating separation of grains and the nature of crack propagation (intergranular). (d) Micrograph taken outside the SCG region.

higher temperatures ($> 1000°$ C), the fracture load decreases (Fig. 4) concomitant with a change in crack growth mechanism as shown later.

At 1200° C, σ_F decreased abruptly (Fig. 4) and the fracture surface showed a localized SCG region as the failure zone (Fig. 5a). The slow crack growth region ACB in Fig. 5a is distinct in its appearance, being characterized by a rough surface (Fig. 5b). The mode of fracture during SCG is primarily intergranular (Fig. 5c), and outside the SCG region it is a mixture of transgranular and intergranular crack propagation (Fig. 5d). The transition from an intergranular mode of SCG to a transgranular cleavage mode accompanying high-speed fracture indicates that a fine balance exists between the alternate crack paths. In high-speed fracture, plastic deformation integral to crack growth is minimized due to the very high strain rate in the vicinity of the crack tip, and the crack finds a transgranular path easier than a more deformation-accommodating grain boundary region. During SCG, the crack extends by plastic separation of what appears to behave as a ductile, low viscosity grain boundary glass phase, at stress levels considerably less than that necessary to promote transgranular fast fracture. When the stress intensity at the tip of the crack has increased sufficiently due to crack lengthening by SCG, a point is reached beyond which fast, transgranular fracture is more favourable (the Griffith condition is satisfied) and a transition to high speed catastrophic fracture occurs as in Fig. 5. The high temperature deformation behaviour (especially the nature and morphology of crack propagation during SCG) of SNW–1000 has many similarities to lithium–aluminium–silicate glass–ceramic [10] and MgO-doped hot-pressed silicon nitride [11].

Up to 1200° C, the load–deflection curves showed linear elastic behaviour (Fig. 6a), and at

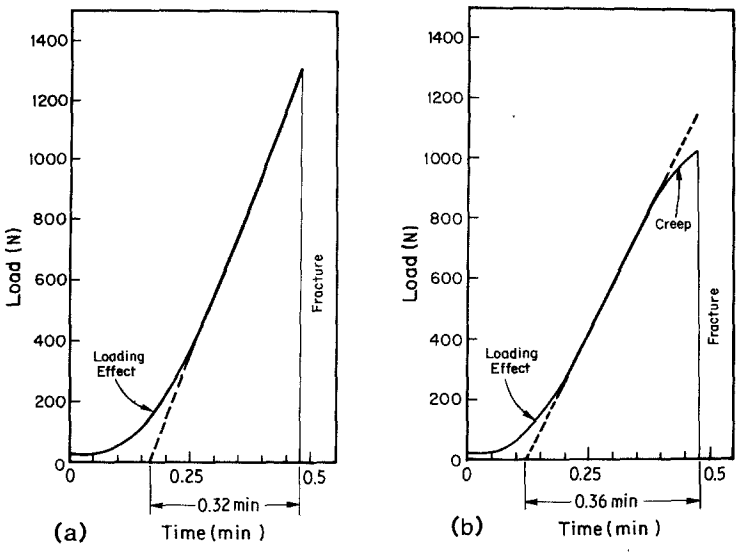

Figure 6 Typical traces of load–deflection curves for specimens tested in four-point bending at (a) 1200° C and (b) 1300° C. Note the deviation from the linear (elastic) portion of the curve at 1300° C due to extensive viscous flow (glass softening). Fracture loads 1320 and 1020 N for (a) and (b) respectively.

1300° C significant deviation from the elastic line was noted, indicative of creep deformation (Fig. 6b). Examination of the fracture surface revealed a large region of SCG (Fig. 7a), and extensive viscous flow due to glass formation causing smearing of grains is clearly visible (Fig. 7b). The remainder of the fracture surface (outside the SCG zone) also displayed glass smearing effects (Fig. 7c). Note that the microstructure in this material consists of equiaxed, fine-grained (1 to 3 μm) and some acicular structure (Fig. 5c). The large decrease in σ_F both at 1200° and 1300° C relative to the σ_F at 20° C, and large viscous flow at high temperatures ($\geqslant$ 1000° C), both suggest that SNW–1000 contained large amounts (2 to 3 wt %) of alumina.

3.3. Flexural stress rupture

It should be pointed out that yttria-doped silicon nitride consolidated in a hot-pressed or sintered condition shows severe degradation of strength at low temperatures (600 to 1000° C) [4–8, 12, 13] due to both static oxidation and

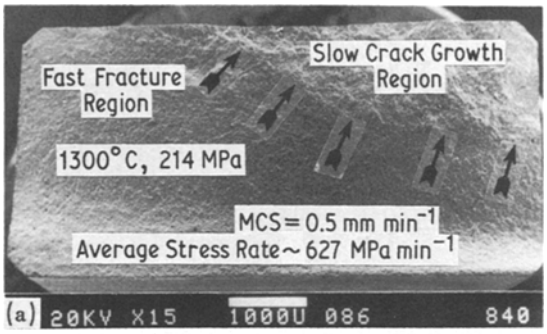

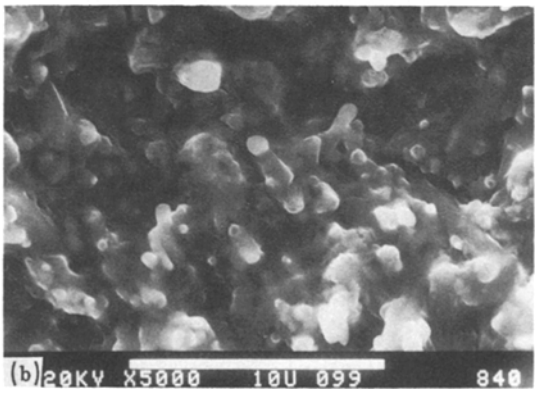

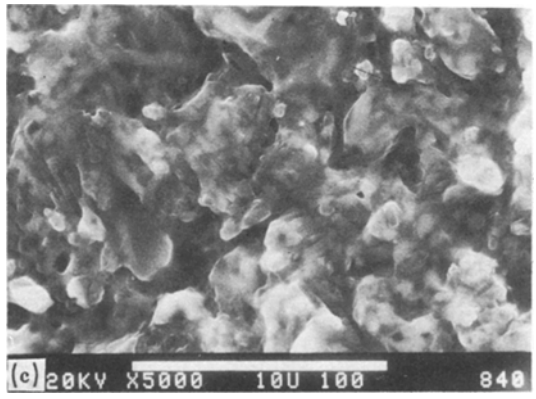

Figure 7 Typical fracture surface as seen in SEM. (a) Large region of SCG followed by a fast-fracture (smooth surface region. (b) Micrograph taken inside the SCG region showing grain separation and void formation due to grain boundary sliding. (c) Micrograph taken outside the SCG region, showing smearing of grains due to viscous flow of glassy material.

TABLE I Flexural-stress rupture results for yttria-doped sintered silicon nitride SNW–1000

Specimen number	Test temperature (° C)	Applied stress (MPa)	Failure time (h)	Sustained time without failure (h)	Fracture origin, oxidation region, discoloration* and bending of specimen
1	800	276	–	140	No discoloration and bending
2	800	344	–	100	No visible discoloration
3	800	344	–	164	No visible discoloration
4	800	344	–	164	No visible discoloration
5	800	413	0.6	–	Porosity, no visible SCG
6	800	413	2.7	–	Porosity, no visible SCG
7	800	413	–	216	No discoloration and bending
8	1000	207	–	100	Grey to white, no visible bending
9	1000	262	–	104	Grey to white, no visible bending
10	1000	262	12.3	–	Porosity and SCG region
11	1000	276	1.7	–	Inclusion and SCG region (Fig. 8)
12	1000	276	5.5	–	Surface porosity and limited SCG
13	1000	276	8.0	–	Porosity and SCG region
14	1000	344	0.6	–	Specimen failed from corner
15	1100	276	0.05	–	Specimen failed from corner
16	1100	276	–	100	Grey to white, fine surface bending
17	1100	276	–	120	Grey to white, fine surface bending
18	1100	344	Instant	–	Corner failure, grey to white
19	1200	276	0.016	–	Corner failure, grey to white
20	1200	276	0.032	–	Corner failure, grey to white

*As-processed material is light grey.

stress-enhanced oxidation. Therefore, flexural stress rupture tests were carried out as a function of temperature (800 to 1200° C) and applied stress in order to determine (a) the material's susceptibility for low temperature instability, (b) the presence of SCG at high temperatures (1000 to 1200° C), and (c) to identify allowable stress levels for limited time ($\leqslant 100$ h). A total of 20 specimens were tested in the flexural stress rupture mode and the results are summarized in Table I. At an applied stress level of 413 MPa and 800° C, three specimens were tested. Two of them failed in 0.6 and 2.7 h and the third specimen sustained 216 h without failure. Fracture surfaces for these failed specimens showed porosity at the failure site, and no signs of SCG were visible. As the applied stress was decreased to 344 MPa, specimens sustained the stress for over 150 h and did not show any visible signs of degradation such as discolouration, isolated spot or patch appearance, and bending. At 800° C, it is believed that oxidation did not play a significant role in causing failures due to two reasons: (a) no significant weight gains were observed among those specimens (Nos. 1 to 4 and 7) which survived over 100 h duration; and (b) fracture surfaces did not reveal penetration of localized or preferential oxygen diffusion areas suggesting oxide-related failures. The specimen which sustained 216 h without failure shows that SNW–1000 is capable of sustaining high stress levels, provided that processing and fabrication flaws can be controlled.

At 1000° C, the material showed a distinctly different behaviour than that seen at 800° C. At low stress levels (~ 200 MPa), the material was able to withstand the stress for periods of 100 h without showing signs of degradation. As the stress was increased to 276 MPa, the time to failure decreased drastically as displayed by three specimens failing in 1.7, 5.5 and 8.0 h, respectively. All three specimens showed a failure initiation site, followed by a region of SCG. A typical fracture surface for the specimen failing in 1.7 h (Fig. 8) clearly shows the large inclusion as the failure initiation site (Fig. 8a), leading to a subsequent SCG region as revealed in SEM micrographs (Figs. 8b and c). Examin-

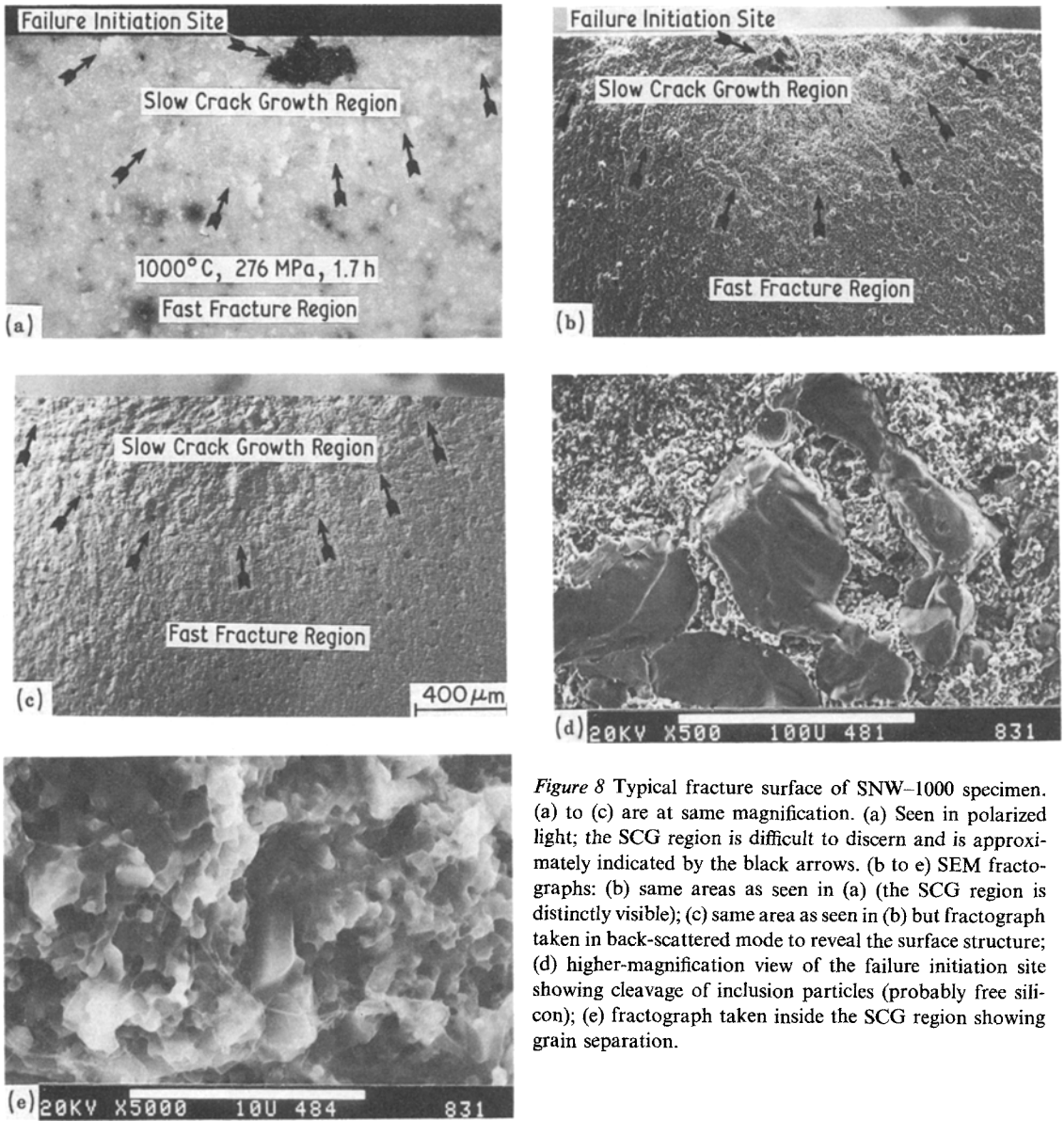

Figure 8 Typical fracture surface of SNW–1000 specimen. (a) to (c) are at same magnification. (a) Seen in polarized light; the SCG region is difficult to discern and is approximately indicated by the black arrows. (b to e) SEM fractographs: (b) same areas as seen in (a) (the SCG region is distinctly visible); (c) same area as seen in (b) but fractograph taken in back-scattered mode to reveal the surface structure; (d) higher-magnification view of the failure initiation site showing cleavage of inclusion particles (probably free silicon); (e) fractograph taken inside the SCG region showing grain separation.

ation of the inclusion at higher magnification (Fig. 8d) revealed that it consisted of several particles* or grains which cleaved under stress, and subsequent crack propagation around the grains is visible. The intergranular nature of crack propagation during SCG is characterized by grain separation, void or cavity formation, and smearing of grains due to viscous flow of glass (Fig. 8e). Some fibrous structure was also observed (Fig. 8e). As the stress was increased to 344 MPa, failure occurred in a short time (0.6 h).

At temperatures above 1000° C the material was incapable of sustaining stress levels of 344 MPa, and showed instant failures. At 276 MPa, three specimens were tested at 1100° C; two sustained the stress without failure for 100 and 120 h and showed fine surface bending, suggesting the onset of creep. The third specimen failed in 3 min (Table I). Failure appeared to have originated from the corner. At 1200° C, the magnitude of 276 MPa applied stress was too high and failures occurred in very short durations, 1 min and 2 min respectively.

*It appears that these grains are unreacted free silicon particles, as suggested by smooth cleaved faces, which were possibly picked up as processing contaminants.

4. Summary

The flexural strength is independent of temperature from 20 to 900° C. The mode of crack propagation in this temperature range is primarily transgranular. The subsequent increase in fracture strength at 1000° C (range 950 to 1050° C) appears attributable to blunting of the flaws due to early stages of viscous flow of the glassy phase in the material. Above 1000° C, the fracture strength decreased significantly due to the presence of extensive subcritical crack growth as a result of creep deformation.

Flexural stress rupture tests at 800 and 1000° C indicated that the material can sustain 200 and 150 MPa without failure for a limited time ($\leqslant$ 100 h), respectively. Above 1000° C the material is unstable and shows creep deformation.

Acknowledgements

The author is thankful to L. Swank for supplying the test specimens, R. Allor for testing ten specimens at 20° C, and R. Goss for scanning electron microscopy.

References

1. C. L. QUACKENBUSH and J. L. SMITH, "GTE Sintered Silicon Nitride", Paper No. 84-GT-228, ASME Gas Turbine Meeting, March 1984.
2. R. K. GOVILA, Technical Report TR 80-18 (Army Materials and Mechanics Research Center, Watertown, Massachusetts, 1980).
3. R. K. GOVILA, J. A. HERMAN and N. ARNON, "Stress Rupture Test Rig Design for Evaluating Ceramic Material Specimens," Paper No. 85-GT-181, ASME Gas Turbine Meeting, 18–21 March, 1985, Houston, Texas.
4. J. T. SMITH and C. L. QUACKENBUSH, *Amer. Ceram. Soc. Bull.* **59** (1980) 529.
5. C. L. QUACKENBUSH and C. L. SMITH, *ibid.* **59** (1980) 533.
6. F. L. LANGE, *ibid.* **62** (1983) 369.
7. R. R. WILLS, S. HOLMQUIST, J. M. WIMMER and J. A. CUNNINGHAM, *J. Mater. Sci.* **11** (1976) 305.
8. F. F. LANGE, S. C. SINGHAL and R. C. KUZNICKI, *J. Amer. Ceram. Soc.* **60** (1977) 249.
9. T. E. EASLER, R. C. BRADT and R. E. TRESSLER, *ibid.* **65** (1982) 317.
10. R. K. GOVILA, K. R. KINSMAN and P. BEARDMORE, *J. Mater. Sci.* **13** (1978) 2081.
11. *Idem, ibid.* **14** (1979) 1095.
12. K. W. BENN and W. D. CARRUTHERS, Third Quarterly Program Report, NASA Contract DEN 3-27 (Air Research Mfg Co of Arizona, 1978) p. 15.
13. R. K. GOVILA, J. A. MANGELS and J. R. BAER, *J. Amer. Ceram. Soc.* **68** (1985) 413.

Received 12 November
and accepted 28 November 1984